J. Fluid Mech. (1989), vol. 202, pp. 295–317
Printed in Great Britain

Spectral approach to non-isotropic turbulence subjected to rotation

By C. CAMBON† AND L. JACQUIN‡

† Laboratoire de Mécanique des Fluides et d'Acoustique, UA CNRS no. 63, Ecole Centrale de Lyon, Ecully, France

‡ Office National d'Etudes et de Recherches Aérospatiales, Chatillon, France

(Received 7 July 1986 and in revised form 16 December 1988)

The non-isotropic effects of solid-body rotation on homogeneous turbulence are investigated in this paper. A spectral formalism using eigenmodes introduces the spectral Coriolis effects more easily and leads to simpler expressions for the integral quadratic terms which come mostly from classical two-point closures. The analysis is then applied to a specific eddy damped quasi-normal Markovian model, which includes the inertial waves regime in the evaluation of triple correlations. This procedure allows for a departure from isotropy by external rotation effects. When started with rigorously isotropic initial data, the various trends observed on the Reynolds stresses and the integral lengthscales remain in accordance with the results from direct simulations; moreover they reflect a very specific spectral angular distribution. Such an angular dependence allows a drain of spectral energy from the parallel to the normal wave vectors (with respect to the rotation axis), and thus appears consistent with a trend toward two-dimensionality.

1. Introduction

Among the different aspects of motion in rotating fluids, the influence of Coriolis effects on the dynamics of an homogeneous turbulent field is not well understood. When one considers the experiments already done in this area, the information available is scarce and even contradictory. This fact is due especially to the great difficulties one encounters when trying to simulate an ideal configuration in a laboratory. Several experiments have been performed in rotating tanks with different forcing systems (see e.g. Hopfinger, Browand & Gagne 1983 for a review of these experiments). Most of them were aimed at obtaining a stationary quasi-two-dimensional flow in the tank, as predicted by the Proudman theorem, and investigate some fundamental properties of the quasi-geostrophic state, a state which is encountered in geophysical flows. However, before their transition to this asymptotic state, the flows were generally not homogeneous, and the mechanisms involved there were certainly far outside the frame of homogeneous turbulence.

The only experiment that seems to have entered this homogeneous framework is that by Wigeland (1978) in which a uniform flow was set into solid-body rotation as it passed through both a rotating honeycomb and a rotating turbulence-generating grid. By these means a satisfactory homogeneous field was obtained with small Rossby numbers. This experiment, because of its underlying principle, focused on the first stages of the effects of a strong rotation on an initially three-dimensional state, which in this case would be essentially a classical grid-generated turbulence. The main results obtained in these experiments showed that the rotation slowed the

kinetic energy decay and increased the lengthscales as well as increasing their departures from isotropic relations. These results have been predicted by numerical simulations (see Bardina, Ferziger & Rogallo 1985; Dang & Roy 1985). Despite the increasing anisotropy of the lengthscales, the Reynolds stress tensor remains nearly spherical (equality of the three principal components) in the simulations. Thus the anisotropy of the flow is masked if one considers only the departure from sphericity of the Reynolds stress tensor. It is therefore necessary to account for the distribution in wave space, or, equivalently, the second-order spectral tensor. This last contains the most detailed information about the anisotropy, and makes it possible to retrieve by integration all the statistical quantities, including integral lengthscales and Reynolds stress components. Moreover, an understanding of the underlying mechanisms is of fundamental importance when considering the problem of the transition from strongly three-dimensional turbulence to a quasi-two-dimensional flow dominated by rotation. Numerical simulations have not yet brought decisive information to this situation. The present analysis intends to delve further into this problem.

First, in order to overcome the difficulties encountered in modelling the effects of the Coriolis force, it will be useful to complement and improve the present formulations (Batchelor 1953; Craya 1958; and Herring 1974 among others) in order to have 'a sufficiently highly structured mathematical level to deal with the subtleties of the problem' (Herring).

Starting from a pure isotropic state, rotation acts only through nonlinear interactions. Considering the set of statistical equations governing the correlations of any order, these nonlinear interactions are accounted for by the triple correlation if one looks at the double correlations. In the presence of rotation, linearized equations exhibit a regime of waves called inertial waves. Cambon (1982), Cambon, Teissèdre & Jeandel (1985) and Cambon & Jacquin (1985) have shown how this linear wave regime influences the velocity correlations of any order. Section 2 summarizes the procedures adopted. In spectral space, the kernels of the associated linear operators are generated by products of the rotation matrix around the wave vector, and it thus appears convenient to work with corresponding eigenmodes. This formulation takes into account, in a simple way, the dispersive and non-isotropic properties of the inertial waves; it also exhibits specific effects of rotation coming in through the third-order moment equation.

The spectral approach allows one to accurately separate pure linear and nonlinear mechanisms. The latter are accounted for through a model for the triple correlations. This model is based on an eddy damped quasi-normal Markovian (EDQNM) assumption, which retains the non-isotropic structure of the operators together with a damping rate chosen according to standard procedures.

The pure linear effects influence the double correlations only if one considers an initially non-isotropic state. These effects are preliminarily analysed in §3, where the triple correlations are ignored in the evolution of the double correlations. Particular non-isotropic initial conditions are generated by solutions of rapid-distortion equations. The corresponding evolution of Reynolds stress tensors and integral lengthscales are studied, and the detailed relationship between physical and spectral quantitities is also given.

In §4, the nonlinear interactions are illuminated by application to the model problem, which starts with an isotropic initial condition. In this case, the departure from isotropy of double correlation is, at least in a preliminary phase, only governed by triple correlations. Results concerning the evolution of the Reynolds stress tensor

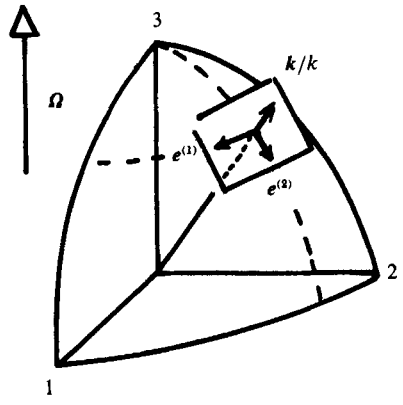

FIGURE 1. Sketch of a sphere of radius k and local frame attached to $\boldsymbol{k}$.

and the lengthscales are presented. Through an extensive analysis of spectral quantities, some fundamental mechanisms underlying the observed trends are illuminated. The trends towards two-dimensionality are discussed in §5.

2. Formalism for non-isotropic homogeneous turbulence

2.1. *Kinematics of the fluctuating field*

Let $\boldsymbol{u}(\boldsymbol{x},t)$ be a statistically homogeneous velocity field. When considering homogeneous incompressible flows, it is convenient to work with the Fourier transform of $\boldsymbol{u}$ defined by

$$\hat{\boldsymbol{u}}(\boldsymbol{k},t) = \frac{1}{(2\pi)^3}\int \boldsymbol{u}(\boldsymbol{x},t)\exp(-\mathrm{i}\boldsymbol{k}\cdot\boldsymbol{x})\,\mathrm{d}^3\boldsymbol{x}; \quad \mathrm{i}^2 = -1.$$

The condition of incompressibility implies that the complex vector $\hat{\boldsymbol{u}}$ is located in the plane $P_{\boldsymbol{k}}$ normal to the wave vector $\boldsymbol{k}$, and the following decomposition (Herring 1974) may be used:

$$\hat{\boldsymbol{u}}(\boldsymbol{k},t) = u'_\alpha(\boldsymbol{k},t)\,\boldsymbol{e}^{(\alpha)}(\boldsymbol{k}); \quad \alpha = 1,2.$$

The vectors $\boldsymbol{e}^{(1)}$ and $\boldsymbol{e}^{(2)}$, characterizing the local frame, are

$$\boldsymbol{e}^{(1)}(\boldsymbol{k}) = \frac{\boldsymbol{k}\times\boldsymbol{\Omega}}{|\boldsymbol{k}\times\boldsymbol{\Omega}|}, \quad \boldsymbol{e}^{(2)}(\boldsymbol{k}) = \frac{\boldsymbol{k}\times\boldsymbol{e}^{(1)}(\boldsymbol{k})}{|\boldsymbol{k}\times\boldsymbol{e}^{(1)}(\boldsymbol{k})|}$$

(see figure 1). Here the summation convention is implied; italic indices take the values 1, 2, 3 and greek indices take values 1 and 2 only.

In order to have a simpler formulation of the change of local frame (rotation of angle φ_0 in the $P_{\boldsymbol{k}}$ plane), it is convenient to use the following complex form:

$$\boldsymbol{N}(\boldsymbol{k}) = \boldsymbol{e}^2(\boldsymbol{k}) - \mathrm{i}\boldsymbol{e}^{(1)}(\boldsymbol{k}); \quad \boldsymbol{N}^*(\boldsymbol{k}) = \boldsymbol{e}^{(2)}(\boldsymbol{k}) + \mathrm{i}\boldsymbol{e}^{(1)}(\boldsymbol{k}) = \boldsymbol{N}(-\boldsymbol{k}).$$

$\boldsymbol{N}$, $\boldsymbol{N}^*$ and $\boldsymbol{k}$ are thus the eigenvectors of the rotation matrix $\boldsymbol{R}$, which has $\boldsymbol{k}$ for its axis and φ_0 for its angle, according to the following intrinsic expression:

$$\boldsymbol{R}(\boldsymbol{k}/k,\varphi_0) = \tfrac{1}{2}(\boldsymbol{N}(\boldsymbol{k})\otimes\boldsymbol{N}(-\boldsymbol{k})\cdot\mathrm{e}^{\mathrm{i}\varphi_0(\boldsymbol{k})} + \boldsymbol{N}(-\boldsymbol{k})\otimes\boldsymbol{N}(\boldsymbol{k})\cdot\mathrm{e}^{-\mathrm{i}\varphi_0(\boldsymbol{k})}) + \frac{\boldsymbol{k}\otimes\boldsymbol{k}}{k^2}.$$

Note that the decomposition in terms of 'helicity waves' proposed by Lesieur (1972) introduced the complex vector $\boldsymbol{N}(\boldsymbol{k})\mathrm{e}^{\mathrm{i}\boldsymbol{k}\cdot\boldsymbol{x}}$ as an eigenvector of the curl operator.

In the case of a solenoidal field ($\boldsymbol{u}$ non-divergent), $\boldsymbol{R}$ reduces to the following projection rotation operator:

$$\boldsymbol{G}(\boldsymbol{k}/k,\varphi_0)=\tfrac{1}{2}(\boldsymbol{N}(\boldsymbol{k})\otimes\boldsymbol{N}(-\boldsymbol{k})\,\mathrm{e}^{\mathrm{i}\varphi_0(\boldsymbol{k})}+\boldsymbol{N}(-\boldsymbol{k})\otimes\boldsymbol{N}(\boldsymbol{k})\,\mathrm{e}^{-\mathrm{i}\varphi_0(\boldsymbol{k})}), \tag{1}$$

which characterizes any change of the local frame. For $\varphi_0=0$, the classical projector $P_{ij}(\boldsymbol{k})=\delta_{ij}-k_ik_j/k^2$ is recovered.

Two corresponding components ζ_ϵ, whose moduli are invariant can be substituted for the u'_α, so that

$$\hat{\boldsymbol{u}}(\boldsymbol{k},t)=\zeta_{+1}(\boldsymbol{k},t)\,\boldsymbol{N}(\boldsymbol{k})+\zeta_{-1}(\boldsymbol{k},t)\,\boldsymbol{N}(-\boldsymbol{k})=\sum_{\epsilon=\pm1}\zeta_\epsilon(\boldsymbol{k},t)\,\boldsymbol{N}(\epsilon\boldsymbol{k}). \tag{2}$$

Considering now the governing equations, the velocity field $\boldsymbol{u}(\boldsymbol{x},t)$ satisfies the Navier–Stokes equation including the Coriolis force term. The corresponding equation in spectral space is written as follows:

$$\left(\frac{\partial}{\partial t}+\nu k^2\right)\hat{u}_i(\boldsymbol{k},t)+2\boldsymbol{\Omega}\cdot\boldsymbol{k}/k\epsilon_{ijl}\frac{k_j}{k}\hat{u}_l(\boldsymbol{k},t)=-\mathrm{i}P_{im}(\boldsymbol{k})\,k_l\int\hat{u}_l(\boldsymbol{p},t)\,\hat{u}_m(\boldsymbol{q},t)\,\mathrm{d}^3\boldsymbol{p},$$

where ν is the kinematic viscosity, ϵ_{ijl} the antisymmetric Ricci tensor and the integral is performed according to the selection rule $\boldsymbol{p}+\boldsymbol{q}=\boldsymbol{k}$.

Using the new variables ζ_ϵ, it is found that

$$\left(\frac{\partial}{\partial t}+\nu k^2-2\mathrm{i}\boldsymbol{\Omega}\cdot\frac{\boldsymbol{k}}{k}\right)\zeta_\epsilon(\boldsymbol{k},t)=\sum_{\substack{\epsilon'=\pm1\\ \epsilon''=\pm1}}-\tfrac{1}{2}\mathrm{i}\int[\boldsymbol{k}\cdot\boldsymbol{N}(\epsilon'\boldsymbol{p})]\,[\boldsymbol{N}(-\epsilon\boldsymbol{k})\cdot\boldsymbol{N}(\epsilon''\boldsymbol{q})]\,\zeta_{\epsilon'}(\boldsymbol{p},t)\,\zeta_{\epsilon''}(\boldsymbol{q},t)\,\mathrm{d}^3\boldsymbol{p}. \tag{3}$$

This basic equation may be formally analysed as a model for the statistical equation (having a similar structure) obtained by the two-point closures. If the right-hand side of (3) is ignored, the following relation characterizes the linear wave regime completely:

$$\zeta_\epsilon(\boldsymbol{k},t)\exp(\mathrm{i}\boldsymbol{k}\cdot\boldsymbol{x})=\exp\left[\mathrm{i}\left(\boldsymbol{k}\cdot\boldsymbol{x}+2\epsilon\boldsymbol{\Omega}\cdot\frac{\boldsymbol{k}}{k}t\right)\right]\zeta_\epsilon(\boldsymbol{k},0);\quad\epsilon=\pm1,\quad\nu=0,$$

where the ζ_ϵ are the eigenmodes and $2\boldsymbol{\Omega}\cdot\boldsymbol{k}/k^2$ is the phase speed. In the fixed frame of reference, the corresponding relation displays the kernel by using the matrix $\boldsymbol{G}$ (relation (1)):

$$\hat{\boldsymbol{u}}(\boldsymbol{k},t)=\boldsymbol{G}\left(\frac{\boldsymbol{k}}{k},2\boldsymbol{\Omega}\cdot\frac{\boldsymbol{k}}{k}t\right)\cdot\hat{\boldsymbol{u}}(\boldsymbol{k},0). \tag{4}$$

On the right-hand side of (3), it is convenient to separate in the triadic integral the terms depending only on the triad geometry and the terms depending also on the angular position of the plane containing $\boldsymbol{k},\boldsymbol{p},\boldsymbol{q}$. Using the local frames introduced by Craya (1958), who considered the triadic system in connection with the triple correlations, one finds the following expression:

$$\left(\frac{\partial}{\partial t}+\nu k^2-2\mathrm{i}\boldsymbol{\Omega}\cdot\frac{\boldsymbol{k}}{k}\right)\zeta_\epsilon(\boldsymbol{k},t)=\sum_{\substack{\epsilon'=\pm1\\ \epsilon''=\pm1}}\iint_{\Delta_k}\mathrm{d}p\,\mathrm{d}q\,m_{\epsilon\epsilon'\epsilon''}(k,p,q)$$
$$\times\int_0^{2\pi}\mathrm{d}\lambda\exp[-\mathrm{i}(\epsilon\lambda+\epsilon'\lambda'+\epsilon''\lambda'')]\,\zeta_{\epsilon'}(\boldsymbol{p},t)\,\zeta_{\epsilon''}(\boldsymbol{q},t), \tag{5}$$

where k,p,q are the moduli of the vectors and $\lambda,\lambda',\lambda''$ denote the angles of rotation of the plane $(\boldsymbol{k},\boldsymbol{p},\boldsymbol{q})$ respectively around $\boldsymbol{k},\boldsymbol{p}$, and $\boldsymbol{q}$. Δ_k is the domain of p and q so

that $\boldsymbol{k}+\boldsymbol{p}+\boldsymbol{q}=\boldsymbol{0}$. In the complex formalism used above, $\lambda, \lambda', \lambda''$ are phases, accurately defined as follows:

$$\boldsymbol{N}(\boldsymbol{k}) = \mathrm{e}^{\mathrm{i}\lambda}(\boldsymbol{\beta}+\mathrm{i}\boldsymbol{\gamma}), \quad \boldsymbol{N}(\boldsymbol{p}) = \mathrm{e}^{\mathrm{i}\lambda'}(\boldsymbol{\beta}'+\mathrm{i}\boldsymbol{\gamma}), \quad \boldsymbol{N}(\boldsymbol{q}) = \mathrm{e}^{\mathrm{i}\lambda''}(\boldsymbol{\beta}''+\mathrm{i}\boldsymbol{\gamma}),$$

where $(\boldsymbol{\beta}, \boldsymbol{\gamma})$, $(\boldsymbol{\beta}', \boldsymbol{\gamma})$ and $(\boldsymbol{\beta}'', \boldsymbol{\gamma})$ are the triadic Craya local frames, attached to $\boldsymbol{k}, \boldsymbol{p}, \boldsymbol{q}$ respectively, so that $\boldsymbol{\gamma}$ is normal to the plane containing $(\boldsymbol{k}, \boldsymbol{p}, \boldsymbol{q})$.

2.2. *Two-point correlations*

Now, extending the formalism to kinematics of the second-order ensemble mean moments of $\boldsymbol{u}$, we introduce the second-order spectral tensor $\hat{U}_{ij}(\boldsymbol{k}, t)$:

$$\langle \hat{u}_i^*(\boldsymbol{p}, t)\, \hat{u}_j(\boldsymbol{k}, t)\rangle = \hat{U}_{ij}(\boldsymbol{k}, t)\, \delta(\boldsymbol{k}-\boldsymbol{p}).$$

Then, using the previous local frame, we write

$$\hat{U}_{ij}(\boldsymbol{k}, t) = \phi'_{\alpha\beta}(\boldsymbol{k}, t)\, \mathrm{c}_i^{\alpha}(\boldsymbol{k})\, \mathrm{e}_j^{\beta}(\boldsymbol{k}).$$

Note that for a particular choice of the polar direction ($\Omega_i = \Omega\delta_{i3}$), the four components of $\Phi'_{\alpha\beta}$ give the four 'basic scalars' of Craya (1958). Hence, we prefer to use linear combinations having invariance properties in considering an arbitrary change of the local frame. So the relation (2) leads to

$$\hat{U}_{ij}(\boldsymbol{k}, t) = e(\boldsymbol{k}, t)\, P_{ij}(\boldsymbol{k}) + \mathrm{Re}\,[z(\boldsymbol{k}, t)\, N_i(\boldsymbol{k})\, N_j(\boldsymbol{k})] + \mathrm{i}\frac{h(\boldsymbol{k}, t)}{k}\epsilon_{ijl}\frac{k_l}{k}. \tag{6}$$

Here $e, |z|, h$ are invariants of the spectral tensor $\hat{U}_{ij}(\boldsymbol{k}, t)$: $e(\boldsymbol{k}, t)$ is the (full three-dimensional) energy spectrum, defined by

$$e(\boldsymbol{k}, t) = \tfrac{1}{2}\hat{U}_{ii}(\boldsymbol{k}, t) = \tfrac{1}{2}\phi'_{\alpha\alpha}(\boldsymbol{k}, t)$$

with

$$q(t) = \tfrac{1}{2}\langle \boldsymbol{u}(\boldsymbol{x}, t)\cdot\boldsymbol{u}(\boldsymbol{x}, t)\rangle = \int e(\boldsymbol{k}, t)\, \mathrm{d}^3\boldsymbol{k};$$

$h(\boldsymbol{k}, t)$ is the helicity spectrum

$$h(\boldsymbol{k}, t) = -\tfrac{1}{2}\mathrm{i}\epsilon_{ijl}\, \hat{U}_{ij}(\boldsymbol{k}, t)\, k_l = -\tfrac{1}{2}\mathrm{i}k(\phi'_{12}(\boldsymbol{k}, t) - \phi'_{21}(\boldsymbol{k}, t))$$

so that

$$\tfrac{1}{2}\langle \boldsymbol{u}(\boldsymbol{x}, t)\cdot \mathrm{curl}\,(\boldsymbol{u}(\boldsymbol{x}, t))\rangle = \int h(\boldsymbol{k}, t)\, \mathrm{d}^3\boldsymbol{k};$$

$z(\boldsymbol{k}, t)$ is a complex deviator whose modulus is yet an invariant

$$z(\boldsymbol{k}, t) = \tfrac{1}{2}\hat{U}_{ij}(\boldsymbol{k}, t)\, N_i(-\boldsymbol{k})\, N_j(-\boldsymbol{k}) = \left(\frac{\phi'_{22}-\phi'_{11}}{2} + \mathrm{i}\frac{\phi'_{12}+\phi'_{21}}{2}\right)(\boldsymbol{k}, t). \tag{7}$$

The symmetric real part of $\hat{U}_{ij}(\boldsymbol{k})$, can be more intrinsically characterized by its real non-zero eigenvalues $\phi^{(1)}(\boldsymbol{k}), \phi^{(2)}(\boldsymbol{k})$ and the angle $\alpha_0(\boldsymbol{k})$ from which is rotated (around $\boldsymbol{k}$) the orthonormal eigenframe (principal axis) with the local frame $(\boldsymbol{e}^{(1)}, \boldsymbol{e}^{(2)})$.

In the orthonormal eigenframe $(\boldsymbol{a}, \boldsymbol{b}, \boldsymbol{k}/k)$, one has

$$\mathrm{Re}\,\hat{\boldsymbol{U}} = \phi^{(1)}\boldsymbol{a}\otimes\boldsymbol{a} + \phi^{(2)}\boldsymbol{b}\otimes\boldsymbol{b}; \quad \phi^{(1)} \geqslant \phi^{(2)} > 0,$$

so that

$$e(\boldsymbol{k}, t) = \frac{\phi^{(1)}(\boldsymbol{k}, t) + \phi^{(2)}(\boldsymbol{k}, t)}{2}; \quad z(\boldsymbol{k}, t) = \frac{\phi^{(1)}(\boldsymbol{k}, t) - \phi^{(2)}(\boldsymbol{k}, t)}{2}\exp\{\mathrm{i}(\pi - 2\alpha_0(\boldsymbol{k}, t))\} \tag{8}$$

Thus z is a measure of the departure from isotropy of $\hat{\boldsymbol{U}}$ in the $P_{\boldsymbol{k}}$ plane, and the ratio $|z|/e$ appears as a spectral parameter analogous to the structural parameter used by Townsend (1954) and Gence & Mathieu (1979). The formalism developed here is available for any anisotropic turbulence: if particular statistical symmetries are

Symmetry	e	z		h	Deviatoric part of the Reynolds stress tensor
		Real part	Imaginary part		
Isotropy	$e(k)$	0	0	0	0
Semi-isotropy	$e(k)$	0	0	$h(k)$	0
Axisymmetry	$e(k,\mu_k)$	$\mathrm{Re}\,z(k,\mu_k)$	0	0	$R(\frac{1}{3}\delta_{ij}-n_i n_j)$
Semi-axisymmetry	$e(k,\mu_k)$	$\mathrm{Re}\,z(k,\mu_k)$	$\mathrm{Im}\,z(k,\mu_k)$	$h(k,\mu_k)$	$R(\frac{1}{3}\delta_{ij}-n_i n_j)$

TABLE 1

considered, the number of variables describing the spectral tensor is reduced as shown in table 1.

With our definition, the prefix 'semi' in the table characterizes an invariance group including only the rotation (no reflectional symmetry). In addition to the classical isotropic case, in the literature there are some attempts to treat (in the framework of two-point closures) semi-isotropy (André & Lesieur 1977), or axisymmetry (Herring 1974). Herring denotes the scalar product μ_k as follows:

$$\mu_k = \boldsymbol{n}\cdot\frac{\boldsymbol{k}}{k},$$

where $\boldsymbol{n} = \boldsymbol{\Omega}/\Omega$. The last symmetry mentioned in table 1 is of great interest when the external rotation is present. In the rotating frame, the set (e, z, h) is governed by the following system of equations:

$$\left.\begin{aligned}\left(\frac{\partial}{\partial t}+2\nu k^2\right)e(\boldsymbol{k},t) &= T_{ii}(\boldsymbol{k},t)+T^*_{ii}(\boldsymbol{k},t),\\ \left[\frac{\partial}{\partial t}+2(\nu k^2-2\mathrm{i}\Omega\mu_k)\right]z(\boldsymbol{k},t) &= [T_{ij}(\boldsymbol{k},t)+T^*_{ij}(\boldsymbol{k},t)]N^*_i(\boldsymbol{k})N^*_j(\boldsymbol{k}),\\ \left(\frac{\partial}{\partial t}+2\nu k^2\right)h(\boldsymbol{k},t) &= -\mathrm{i}\epsilon_{ijl}\,k_l\,[T_{ij}(\boldsymbol{k},t)-T^*_{ij}(\boldsymbol{k},t)].\end{aligned}\right\} \tag{9}$$

The right-hand side of the system depends on the triple correlations through the transfer tensor t_{ij} defined by

$$t_{ij}(\boldsymbol{k},t) = T_{ij}(\boldsymbol{k},t)+T^*_{ji}(\boldsymbol{k},t);\quad T_{ij}(\boldsymbol{k},t) = \tfrac{1}{2}\mathrm{i}k_l\int\langle\hat{u}_l(\boldsymbol{q},t)\,\hat{u}_j(\boldsymbol{k},t)\,\hat{u}_i(\boldsymbol{p},t)\rangle\,\mathrm{d}^3\boldsymbol{p}\,\mathrm{d}^3\boldsymbol{q}. \tag{10}$$

The left-hand side includes both viscous and 'linear' Coriolis effects. Ω can only introduce a coupling between the three previous equations through the closure. In the following section, the generalized transfer tensor T_{ij} will be expressed in terms of the functions of dependent variables using typical closure assumptions.

2.3. *The EDQNM closure*

This theory was proposed by Orszag (1970) and has been extensively used for isotropic turbulence. Following Cambon, Jeandel & Mathieu (1981*a*), Cambon (1982), and Cambon, Teissèdre & Jeandel (1985), the approach is enlarged and the non-isotropic linear operator are accounted for, by considering both second- and third-order correlations. The linear solution (4) takes the symbolic form

$$\hat{u}_t = G_t\,\hat{u}_0.$$

Introducing the nonlinearity as an external term, the complete rate equation governing the fluctuating field $\hat{u}$ is formally solved as follows:

$$\hat{u}_t = G_t\,\hat{u}_0 + \int_0^t G_{t-t'}(\hat{u}\hat{u})_{t'}\,\mathrm{d}t'.$$

The same procedure, applied to the equations governing the correlations, leads to

$$\langle\hat{u}\hat{u}\rangle_t = G_t\,G_t\langle\hat{u}\hat{u}\rangle_0 + \int_0^t G_{t-t'}\,G_{t-t'}\langle\hat{u}\hat{u}\hat{u}\rangle_{t'}\,\mathrm{d}t'$$

for the double correlations, and

$$\langle\hat{u}\hat{u}\hat{u}\rangle_t = G_t\,G_t\,G_t\,\langle uuu\rangle_0 + \int_0^t G_{t-t'}\,G_{t-t'}\,G_{t-t'}\langle\hat{u}\hat{u}\hat{u}\hat{u}\rangle_{t'}\,\mathrm{d}t'$$

for the triple correlations.

Only the last relation is concerned when applying the EDQNM assumptions. First, the fourth-order moments are expressed in terms of second order, as for a normal law:

$$\langle\hat{u}\hat{u}\hat{u}\hat{u}\rangle_{t'} = \Sigma\langle\hat{u}\hat{u}\rangle_{t'}\langle\hat{u}\hat{u}\rangle_{t'} \quad \text{(quasi-normal assumption)}.$$

Then the fourth-order cumulants, neglected above, are taken into account through an eddy damping η, which changes G into G^+:

$$G_t^+ = G_t \exp(-\eta t).$$

Last, the instantaneous value $t' = t$ of the double correlations only is accounted for, in accordance with the Markovian assumption.

Finally, one obtains the following closed relation:

$$\langle\hat{u}\hat{u}\hat{u}\rangle_t = G_t^+\,G_t^+\,G_t^+\langle\hat{u}\hat{u}\hat{u}\rangle_0 + \Sigma\int_0^t (G_{t-t'}^+\,G_{t-t'}^+\,G_{t-t'}^+)\,\mathrm{d}t'\langle\hat{u}\hat{u}\rangle_t\langle\hat{u}\hat{u}\rangle_t. \tag{11}$$

The first term corresponds to a 'linear' (or zero Rossby number) evaluation of the triple correlations; it has only a transient effect, as discussed at the end of §4. So for the sake of simplicity, only the second term will be computed in numerical applications:

$$\langle\hat{u}\hat{u}\hat{u}\rangle_t = \Sigma\left(\int_{-\infty}^t G_{t-t'}^+\,G_{t-t'}^+\,G_{t-t'}^+\,\mathrm{d}t'\right)\langle\hat{u}\hat{u}\rangle_t\langle\hat{u}\hat{u}\rangle_t. \tag{12}$$

In this form, the initial data for triple correlations have been taken at $t = -\infty$ and thus 'forgotten'. Considering the definition (10), the detailed expression of the generalized transfer $T_{ij}(\boldsymbol{k}, t)$ corresponding to the symbolic form (12) becomes

$$\begin{aligned} T_{ij}(\boldsymbol{k},t) = \int_{-\infty}^{t'}\mathrm{d}t'\int_{\boldsymbol{k}+\boldsymbol{p}+\boldsymbol{q}=0}\mathrm{d}^3\boldsymbol{p}\,k_q\,[&G_{jm}^+(\boldsymbol{k},t,t')\,P_{muv}(\boldsymbol{k})\,\underline{G_{in}^+(\boldsymbol{p},t,t')\,\hat{U}_{vn}(\boldsymbol{p},t)}\\ &\times\underline{G_{ql}^+(\boldsymbol{q},t,t')\,\hat{U}_{ul}(\boldsymbol{q},t)} + G_{ql}^+(\boldsymbol{q},t,t')\,P_{luv}(\boldsymbol{q})\\ &\times\underline{G_{jm}^+(\boldsymbol{k},t,t')\,\hat{U}_{um}(\boldsymbol{k},t)}\,\underline{G_{in}^+(\boldsymbol{p},t,t')\,\hat{U}_{vn}(\boldsymbol{p},t)}\\ &+G_{in}^+(\boldsymbol{p},t,t')\,P_{nuv}(\boldsymbol{p})\,\underline{G_{ql}^+(\boldsymbol{q},t,t')\,\hat{U}_{vl}(\boldsymbol{q}t)}\,\underline{G_{jm}^+(\boldsymbol{k},t,t')\,\hat{U}_{im}(\boldsymbol{k},t)}], \end{aligned} \tag{13}$$

with $P_{muv}(\boldsymbol{k}) = \frac{1}{2}(k_u P_{mv}(\boldsymbol{k}) + k_v P_{mu}(\boldsymbol{k}))$.

Such an expression corresponds to a DIA formulation if we take Kraichnan's response tensor for $\boldsymbol{G}^+(\boldsymbol{k},t,t')$ and if we replace the underlined terms of type: $G_{jm}^+(\boldsymbol{k},t,t')\,\hat{U}_{um}(\boldsymbol{k},t)$ by the two-time tensor $\hat{U}_{uj}(\boldsymbol{k},t,t')$ (fluctuation-dissipation theorem).

In the EDQNM2 version, $\boldsymbol{G}^+$ is given by the product of the matrix $\boldsymbol{G}$, (which is also the zeroth order response tensor), and an isotropic damping term, so that

$$\boldsymbol{G}^+(\boldsymbol{k},t,t') = \mathrm{Re}\left[\boldsymbol{N}(\boldsymbol{k})\otimes\boldsymbol{N}(-\boldsymbol{k})\exp\left\{2\mathrm{i}\boldsymbol{\Omega}\cdot\frac{\boldsymbol{k}}{k}(t-t')\right\}\right]\exp\{-\eta(\boldsymbol{k},t)\,(t-t')\}. \quad (14)$$

In the EDQNM1 version, the Coriolis terms are neglected in the rate equation governing the triple correlations and the expression for $\boldsymbol{G}^+$ reduces to

$$\boldsymbol{G}^+(\boldsymbol{k},t,t') = \boldsymbol{P}(\boldsymbol{k})\exp\{-\eta(\boldsymbol{k},t)\,(t-t')\}.$$

Note that the two approaches are discussed by Cambon (1982), and Cambon *et al.* (1985) in the case of turbulence subjected to both the strain and the rotation effects. Retaining the more sophisticated relation (14), and time integrating analytically in (13) we get

$$\int_{-\infty}^{t} G^+_{jm}(\boldsymbol{k},t,t')\,G^+_{in}(\boldsymbol{p},t,t')\,G^+_{ql}(\boldsymbol{q},t,t')\,\mathrm{d}t'$$
$$= \frac{1}{8}\sum_{\substack{\epsilon=\pm1\\ \epsilon'=\pm1\\ \epsilon''=\pm1}} N_j(\epsilon\boldsymbol{k})N_m(-\epsilon\boldsymbol{k})N_i(\epsilon'\boldsymbol{p})N_n(-\epsilon'\boldsymbol{p})N_q(\epsilon''\boldsymbol{q})N_l(-\epsilon''\boldsymbol{q})\,\theta^{\epsilon\epsilon'\epsilon''}_{kpq}(t),$$

where

$$\theta^{\epsilon\epsilon'\epsilon''}_{kpq} = \underbrace{[\eta(k,t)+\eta(p,t)+\eta(q,t)}_{\theta^{-1}_{kpq}} - 2\mathrm{i}\Omega(\epsilon\mu_k+\epsilon'\mu_p+\epsilon''\mu_q)]^{-1}. \quad (15)$$

In the new characteristic times so defined, the classical isotropic relaxation time θ_{kpq} is modified as follows by anisotropic factors, including the solid-body rotation rate and the angular parameters $\mu_k = \boldsymbol{\Omega}\cdot\boldsymbol{k}/\Omega k$; $\mu_p = \boldsymbol{\Omega}\cdot\boldsymbol{p}/\Omega p$; $\mu_q = \boldsymbol{\Omega}\cdot\boldsymbol{q}/\Omega q$:

$$\theta^{\epsilon\epsilon'\epsilon''}_{kpq} = \frac{\theta_{kpq}}{\{1-2\mathrm{i}\Omega\theta_{kpq}(\epsilon\mu_k+\epsilon'\mu_p+\epsilon''\mu_q)\}} \quad (\epsilon=\pm1,\epsilon'=\pm1,\epsilon''=\pm1). \quad (16)$$

A modification of θ_{kpq} by $\boldsymbol{\Omega}$ was also proposed by Holloway & Hendershott (1977) in a simpler two-dimensional case (β-plane).

At this stage, we can express the right-hand side terms in (9) in terms of e, z, h. Detailed calculations have been carried out with zero helicity, since helicity appears in (9) only if it already exists in the initial data. Indeed it can be shown that the tensor T_{ij} deduced from (13) and (14) remains real, together with $\hat{U}_{ij}$. As for the nonlinear term in (5) governing the fluctuating spectra ζ_ϵ, one obtains in the 'influence matrices' an optimal separation between moduli and angles by introducing the three angles $\lambda, \lambda', \lambda''$. The new set of integration variables (p, q, λ) takes the place of (p_1, p_2, p_3), so that

$$\int \mathrm{d}^3\boldsymbol{p} = \iiint \mathrm{d}p_1\,\mathrm{d}p_2\,\mathrm{d}p_3 = \iint_{\Delta_k}\frac{pq}{k}\mathrm{d}p\,\mathrm{d}q\int_0^{2\pi}\mathrm{d}\lambda$$

Applying (13), (15) and (6), the integrands related to $T_{ii}+T^*_{ii}$ and to $(T_{ij}+T^*_{ij})N^*_iN^*_j$ are expressed in terms of quadratic functions of e and z, respectively multiplied by

$\theta^{\epsilon\epsilon'\epsilon''}_{kpq}$ and $\theta^{\epsilon\epsilon'\epsilon''}_{kpq}\exp(-2i\lambda)$. These quadratic terms then appear as a sum of the products of two terms chosen from the following set:

$$e(\boldsymbol{k},t),\quad e(\boldsymbol{p},t),\quad e(\boldsymbol{q},t);$$
$$z(\epsilon\boldsymbol{k},t)\exp(2i\epsilon\lambda),\quad z(\epsilon'\boldsymbol{p},t)\exp(2i\epsilon'\lambda'),\quad z(\epsilon''\boldsymbol{q},t)\exp(2i\epsilon''\lambda''),\quad (17)$$

and weighted by coefficients depending only on k,p,q (through scalar products of vectors generating the specific triadic Craya local frames).

For the sake of brevity,† we give as an example only the structure of the term dependent only on e in the energy transfer:

$$T_{ii}(\boldsymbol{k},t)+T^{*}_{ii}(\boldsymbol{k},t)=\sum_{\substack{\epsilon=\pm1\\ \epsilon'=\pm1\\ \epsilon''=\pm1}}\iint_{\Delta_k}\mathrm{d}p\,\mathrm{d}q\,A(\epsilon k,\epsilon' p,\epsilon'' q)\Big\{\int_0^{2\pi}\mathrm{d}\lambda\,\theta^{\epsilon\epsilon'\epsilon''}_{kpq}$$
$$\times e(\boldsymbol{q},t)\,[e(\boldsymbol{p},t)-e(\boldsymbol{k},t)]+\ldots\Big\}. \quad (18)$$

Note that the angular dependence, which requires a numerical evaluation of the λ-integral, is introduced only by the set (17) and by the times $\theta^{\epsilon\epsilon'\epsilon''}_{kpq}$ for the energy transfer and $\theta^{\epsilon\epsilon'\epsilon''}_{kpq}\exp(-2i\lambda)$ for the anisotropy transfer (nonlinear term in the rate equation governing z). The role of $\theta^{\epsilon\epsilon'\epsilon''}_{kpq}$ appears crucial for the anisotropization mechanisms: forcing $\boldsymbol{\Omega}$ to zero in the transfer terms, $\theta^{\epsilon\epsilon'\epsilon''}_{kpq}$ becomes θ_{kpq} and the present model returns to the EDQNM1 version, which is unable to predict a departure from isotropy in the case of pure rotation.

3. Linear evolution of double correlations

On discarding the nonlinear terms in the closed system (9), the solution takes the following form:

$$\left.\begin{aligned} e(\boldsymbol{k},t) &= e(\boldsymbol{k},0)\exp(-2\nu k^2 t),\\ z(\boldsymbol{k},t) &= z(\boldsymbol{k},0)\exp(-2\nu k^2 t+4i\Omega t\mu_k).\end{aligned}\right\} \quad (19)$$

These equations express the impact of inertial waves on double correlations in spectral space. The pure 'linear' effects of rotation consist in a rotation of the eigen directions with a rate $(4\Omega\mu_k)$ which depends on the orientation of the wave vector $\boldsymbol{k}$ with respect to the rotation axis. When we discard non-linear interactions, the inertial wave regime can influence the three-dimensional structure of energy only if the initial configuration is non-isotropic including a non-zero deviator z.

In order to have a deeper understanding of this problem we have built non-isotropic initial spectra by means of the rapid-distortion theory. Axisymmetric initial data are obtained by considering the effects of an axisymmetric duct on isotropic turbulence. One proceeds in the following way. One assumes that the turbulence is subjected to a constant mean strain rate matrix

$$\begin{pmatrix} D & 0 & 0\\ 0 & D & 0\\ 0 & 0 & -2D\end{pmatrix}$$

during the time t_0.

† A copy of the details of nonlinear interactions can be obtained from either the authors or the editor on request.

A negative value of the strain rate D corresponds to a convergent duct and a positive value to a divergent duct. Using the simplified analytical formulation given by Cambon *et al.* (1985) for rapid-distortion solutions, it is found that

$$e_{\mathrm{L}}(\boldsymbol{k},0)=\tfrac{1}{2}[\phi^1_{\mathrm{L}}(\boldsymbol{k},t_0)+\phi^2_{\mathrm{L}}(\boldsymbol{k},t_0)];\quad z_{\mathrm{L}}(\boldsymbol{k},0)=\tfrac{1}{2}[\phi^2_{\mathrm{L}}(\boldsymbol{k},t_0)-\phi^1_{\mathrm{L}}(\boldsymbol{k},t_0)] \tag{20}$$

with

$$\phi^1_{\mathrm{L}}(\boldsymbol{k},t_0)=\mathrm{e}^{-2Dt_0}\frac{E(K)}{4\pi K^2};\quad \phi^2_{\mathrm{L}}(\boldsymbol{k},t_0)=\mathrm{e}^{2Dt_0}\frac{E(K)}{4\pi k^2},$$

where $E(k)$ denotes the isotropic energy spectrum before the distortion and K the wavenumber modified by the advective effects of the mean field:

$$K^2=k^2[(1-\mu_k^2)\,\mathrm{e}^{2Dt_0}+\mu_k^2\,\mathrm{e}^{-4Dt_0}].$$

For practical applications, the type and the degree of anisotropy are fixed by the sign and the value of the strain coefficient Dt_0. Note that the usual assumption restricts the relevance of the rapid-distortion theory to evolution times short compared with a global typical nonlinear time such as $\tau=q/\bar{\epsilon}$ (here q is the turbulent kinetic energy and $\bar{\epsilon}$ its dissipation rate). However, the validity of the theory also depends on the size of the individual structures. In particular when considering the characteristic nonlinear time as being a turnover time

$$\tau(k)=\left[\int_0^k p^2E(p)\,\mathrm{d}p\right]^{-\frac{1}{2}},$$

the theory may be relevant for small k (large structures), even if the former criterion does not hold.

The rapid-distortion solutions (20) quickly give an unrealistic anisotropy in the larger wavenumber range. By assuming local isotropy in the small scale we propose the following isotropic averaging:

$$\left.\begin{aligned} e(\boldsymbol{k},0)&=e_{\mathrm{L}}(\boldsymbol{k},0)\exp\left\{-\left(\frac{k}{k_{\mathrm{i}}}\right)^2\right\}+\frac{E(k,0)}{4\pi k^2}\left[1-\exp\left\{-\left(\frac{k}{k_1}\right)^2\right\}\right]\\ z(\boldsymbol{k},0)&=z_{\mathrm{L}}(\boldsymbol{k},0)\exp\left\{-\left(\frac{k}{k_{\mathrm{i}}}\right)^2\right\}\end{aligned}\right\} \tag{21}$$

where k_{i} is chosen as the inverse of the integral lengthscale. Our axisymmetric initial data thus generated are more complicated than those used, for example, by Herring (1974), but they have two interesting properties.

First, the property of 'axial isotropy' is ensured when $\boldsymbol{k}$ is parallel to the symmetry axis:

$$\mu_k=\pm 1\Rightarrow z=0.$$

In order to ensure this local vanishing, the angular dependence of z is an essential condition.

Secondly, our procedure allows the initially axisymmetric turbulence generated by a grid to be approached. Generally, such a turbulence is characterized in the first test section by a Reynolds stress tensor of the 'cigar' type, having a longitudinal (streamwise) component greater than the transversal. Thus, considering the possible improvement of the isotropy by means of a convergent duct (Comte-Bellot & Corrsin 1971) together with the reversibility of the straining process, one can expect that for $Dt_0>0$ the initial data fit well with the axisymmetric grid turbulence.

Now, we can analyse the consequences of the linear behaviour through classical one-point correlations. The Reynolds stress tensor is deduced by an integration of $\hat{\boldsymbol{U}}$ in the whole spectral space. In the axi- or semi-axisymmetric case, we are concernced with the two components:

$$\left.\begin{aligned}\overline{u_3^2} &= 2\pi \int_0^\infty k^2\,\mathrm{d}k \int_{-1}^{1} [e(k,\mu,t) + \mathrm{Re}\, z(k,\mu,t)]\,(1-\mu^2)\,\mathrm{d}\mu,\\ \overline{u_1^2} = \overline{u_2^2} &= \pi \int_0^\infty k^2\,\mathrm{d}k \int_{-1}^{1} [e(k,\mu,t)\,(1+\mu^2) - \mathrm{Re}\, z(k,\mu,t)\,(1-\mu^2)]\,\mathrm{d}\mu.\end{aligned}\right\} \tag{22}$$

The integral lengthscales are obtained by plane integrations. Recall that in physical space, the scale $L_{ij,l}$ represents a correlation length in the direction l between two components of the fluctuating velocity referenced by i and j:

$$L_{ij,l} = \frac{1}{\langle u_i u_j \rangle} \int_0^\infty \langle u_i(\boldsymbol{x})\, u_j(\boldsymbol{x}+\boldsymbol{r}) \rangle\,\mathrm{d}r$$

with $r_k = r\delta_{kl}$. For homogeneous turbulence, one has

$$L_{ij,l} = \frac{\pi}{\langle u_i u_j \rangle} \iint \hat{U}_{ij}(\boldsymbol{k},t)\Big|_{k_l=0}\,\mathrm{d}^2\boldsymbol{k}.$$

In our simplified configuration, the scales $L_{ij,3}$ characterized by a longitudinal separation, emphasize the spectral distribution in 'the equatorial plane' ($\mu_k = 0$) and require no angular integration:

$$\left.\begin{aligned}L_{33,3} &= \frac{2\pi^2}{\overline{u_3^2}} \int_0^\infty k\,\mathrm{d}k [e(k,0,t) + \mathrm{Re}\, z(k,0,t)],\\ L_{11,3} &= \frac{\pi^2}{\overline{u_1^2}} \int_0^\infty k\,\mathrm{d}k\,[e(k,0,t) - \mathrm{Re}\, z(k,0,t)].\end{aligned}\right\} \tag{23}$$

Only the scales $L_{ii,1}$ (i not summed) relative to a transversal separation introduce an integration over μ_k:

$$\left.\begin{aligned}L_{33,1} &= \frac{2\pi}{\overline{u_3^2}} \int_0^\infty k\,\mathrm{d}k \int_{-1}^{1} [e(k,\mu,t) + \mathrm{Re}\, z(k,\mu,t)]\,(1-\mu^2)^{\frac{1}{2}}\,\mathrm{d}\mu,\\ L_{11,1} &= \frac{2\pi}{\overline{u_1^2}} \int_0^\infty k\,\mathrm{d}k \int_{-1}^{1} [e(k,\mu,t) - \mathrm{Re}\, z(k,\mu,t)]\,(1-\mu^2)^{-\frac{1}{2}}\,\mathrm{d}\mu.\end{aligned}\right\} \tag{24}$$

Considering the integral relations between two-point (spectral) and one-point correlations, it is now easy to predict the evolution of one-point quantities. Neglecting the viscosity effects for the sake of simplicity, the contribution of the deviator z introduces an oscillating trend through the term $\exp(4\mathrm{i}\Omega t\mu)$, but the integration over μ leads to a damping and the oscillating behaviour vanishes if $\mu = 0$.

The damping already found by Itsweire, Chabert & Gence (1979) in a particular configuration, is linked to the asymptotic behaviour of the integral

$$\int_{-1}^{1} f(\mu) \exp(4\mathrm{i}\Omega t\mu)\,\mathrm{d}\mu$$

(close to a Fourier transform), for large values of the parameter $4\Omega t$. Thus one can expect damped oscillations leading to an asymptotic value (only depending

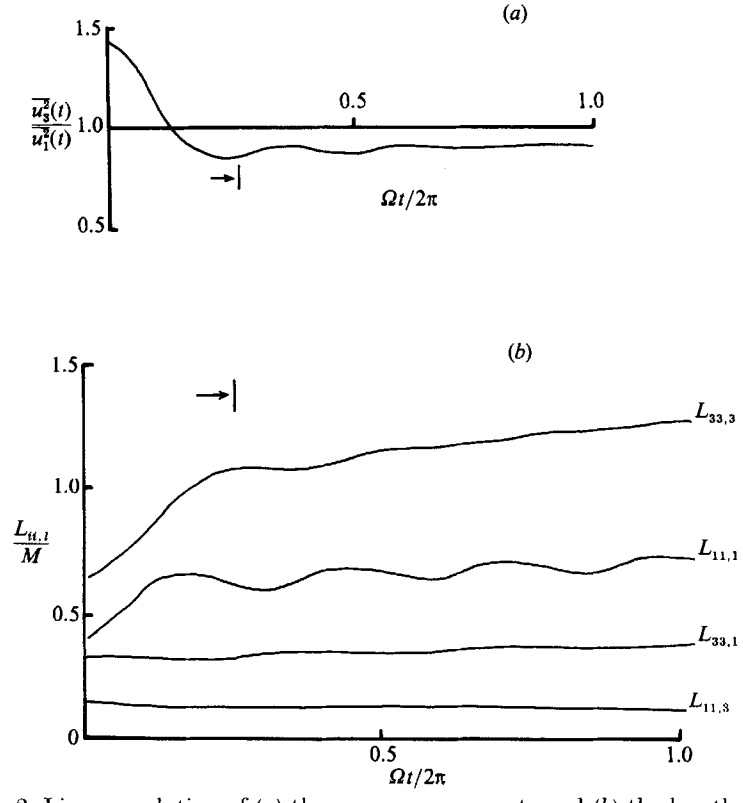

FIGURE 2. Linear evolution of (*a*) the energy components and (*b*) the length-scales for $\Omega = 10\ \mathrm{s}^{-1}$ starting from an axisymmetrically dilated turbulence (rapid distortion).

on $e(k,\mu,0)$ for $\overline{u_1^2}$, $\overline{u_3^2}$, $L_{33,1}$ and $L_{11,1}$, and an evolution controlled only by the weighting factors $1/\overline{u_1^2}$ and $1/\overline{u_3^2}$ for $L_{11,3}$ and $L_{33,3}$.

The case of initial data corresponding to a positive strain $Dt_0 = 0.3$, applied to the spectrum $E(k)$ given by the experiment of Comte-Bellot & Corrsin (1971) at $x/M = 42$ with $M = 5.08$ cm, is presented in figure 2. These data correspond to the flow behind the grid just before the rapid contraction. Figure 2(*a*) shows the behaviour of the ratio between the longitudinal $\overline{u_3^2}$ and the transversal $\overline{u_1^2}$ component of the Reynolds stress tensor. Figure 2(*b*) shows the lengthscales $L_{ii,3}$ and $L_{ii,1}$ (here the viscous damping is taken into account (see (19)). During the first rapid part of the evolution, the Reynolds stress tensor returns towards isotropy, but the anisotropic character of the lengthscales is accentuated. These effects are damped after a quarter of a revolution (see arrow) and an inverse anisotropy for the Reynolds stress tensor is obtained.

The results for $Dt_0 = -0.3$ are presented in Figure 3. Again, the behaviour of $\overline{u_3^2}/\overline{u_1^2}$ corresponds to a rapid return towards isotropy and to a damping at a third of a revolution, with an inverse asymptotic anisotropy. The initial anisotropy of the scales is also accentuated.

These results illustrate the spectacular effect of the inertial wave regime on physical quantities for non-isotropic flows, submitted to rotation.

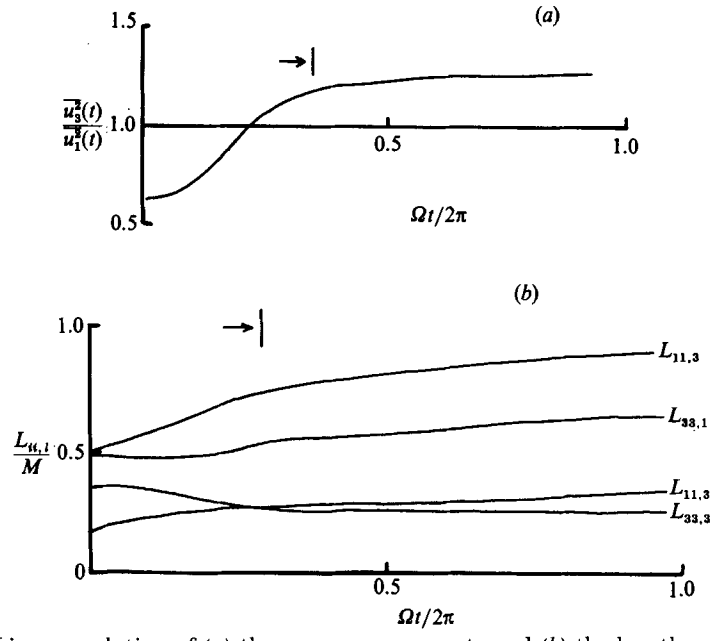

FIGURE 3. Linear evolution of (*a*) the energy components and (*b*) the lengthscales for $\Omega = 10\ \mathrm{s}^{-1}$ starting from an axisymmetrically contracted turbulence (rapid distortion).

	Specific Coriolis parameters	Associated invariants in the linearized equations
Fluctuating field	$2\boldsymbol{\Omega}\cdot\boldsymbol{k}/k$	$\lvert\hat{\boldsymbol{u}}\cdot\boldsymbol{N}\rvert, \lvert\hat{\boldsymbol{u}}\cdot\boldsymbol{N}^*\rvert$
Second-order correlations	$4\boldsymbol{\Omega}\cdot\boldsymbol{k}/k$	$e, \lvert z\rvert, h$
Third-order correlations	$2\boldsymbol{\Omega}\cdot(\boldsymbol{k}/k \pm \boldsymbol{p}/p \pm \boldsymbol{q}/q)$	None

TABLE 2

4. Departure from isotropy

Recall that no effect of Ω is found in the linear terms of the system (9) when the initial deviator is equal to zero. Therefore to ensure departure from isotropy of the double correlations, it appears necessary that the functional relation between $\boldsymbol{T}$ and $\hat{\boldsymbol{U}}$ should be dependent explicitly on Ω. Such a property is satisfied only by the more sophisticated option EDQNM2. The 'Triadic Coriolis parameter'

$$2\boldsymbol{\Omega}\cdot\left(\epsilon\frac{\boldsymbol{k}}{k}+\epsilon'\frac{\boldsymbol{p}}{p}+\epsilon''\frac{\boldsymbol{q}}{q}\right) = 2\Omega(\epsilon\mu_k+\epsilon'\mu_p+\epsilon''\mu_q) \tag{25}$$

takes into account in (15) the wave regime at the level of third-order correlations, and leads to a semi-axisymmetric configuration (see table 1) even if the isotropic form of $\hat{\boldsymbol{U}}$ is introduced in the closure relation. Note that the zero value of these parameters characterizes the resonant constraint identified in the classical Greenspan's (1968) analysis. Ω thus has influence, but for particular configurations of the triad. Table 2 compares the characteristics of the wave regime for different correlations and shows the specificity of the correlations of order greater than two.

Considering the global influence of Ω on one-point correlations, the Rossby number

$$Ro = \frac{1}{2\Omega}\frac{\bar{\epsilon}}{q}; \quad q = \tfrac{1}{2}\langle u_i(\boldsymbol{x},t)\, u_i(\boldsymbol{x},t)\rangle$$

classically compares the timescale $(2\Omega)^{-1}$ associated with the Coriolis effect and a timescale $q/\bar{\epsilon}$ associated with the turbulent field. In our analysis the relevant ratio characterizing the action of rotation is given by

$$\frac{\underbrace{\{\eta(k,t)+\eta(p,t)+\eta(q,t)\}}_{\text{(viscous+eddy) damping}}}{\underbrace{2\Omega(\epsilon\mu_k+\epsilon'\mu_p+\epsilon''\mu_q)}_{\text{triadic Coriolis parameter}}} = \frac{1}{2\Omega\theta_{kpq}(\epsilon\mu_k+\epsilon'\mu_p+\epsilon''\mu_q)}$$

But such a parameter is non-local and non-isotropic. Its impact on the spectral transfer is very hard to predict. It is associated with a specific Rossby number $(2\Omega\theta_{kpq})^{-1}$. Nevertheless, the Rossby number is the first practical criterion for comparing results of different experiments or computations.

Our computations have been carried out in order to solve the closed rate equations governing e and z in the semi-axisymmetric configuration without helicity (see table 1), according to the equations of §2.

For the evaluation of $\theta^{\epsilon\epsilon'\epsilon''}_{kpq}$ (15), the damping coefficient $\eta(k,t)$ is chosen following André & Lesieur (1979):

$$\eta(k,t) = \nu k^2 + A\left[\int_0^k p^2 E(p,t)\,\mathrm{d}p\right]; \quad A = 0.355,$$

where $E(k,t)$ is the classical energy spectrum, obtained by integration of $e(\boldsymbol{k},t)$ over a spherical shell of radius k. The value of A was initially chosen by referring to the test field model results for large values of the turbulent Reynolds number. Cambon *et al.* (1981*a*, *b*) checked the suitability of this choice for predicting several experimental cases of isotropic and even non-isotropic flows (subjected to straining processes) for moderate Reynolds numbers.

In order to preserve the detailed anisotropy, the transfer terms (whose structure is given by (18)) are computed without any assumption about the angular dependence. The λ-integral is computed by a classical discretization method (by using 20 values between 0 and π) and 11 values of μ_k (between 0 and 1) are retained for $e(k,\mu_k,t)$ and $z(k,\mu_k,t)$. Low-order expansions in terms of angular harmonics, such as that used by Herring (1974) seem premature, particularly since the angular dependence of our response tensor (14) is very complicated and this has not been truncated in the present work. The corresponding times $\theta^{\epsilon\epsilon'\epsilon''}_{kpq}$ (15) are thus computed for all the discretized values of k, p, q, μ_k and λ. The standard procedure for evaluating the integral over p and q is not quoted here. As shown by other authors, high Reynolds numbers can be reached by using the logarithmic step (for k, p, q). Consequently, although the fairly important number of angular degrees of freedom, the method requires a reasonable amount of computational time with respect to a direct numerical simulation.

For detailed analysis, a typical computation is chosen, started with rigorously isotropic initial data:

$$e(k,\mu_k,0) = \frac{E(k)}{4\pi k^2}; \quad z(k,\mu_k,0) = h(k,\mu_k,0) = 0,$$

and $E(k)$ is deduced from a classical grid turbulence experiment (Comte-Bellot & Corrsin 1971) having a microscale Reynolds number $R_\lambda = 70$ in the first section.

The initial angular response of the energy transfer $T_e = 4\pi k^2(T_{ii}+T^*_{ii})$ is shown on

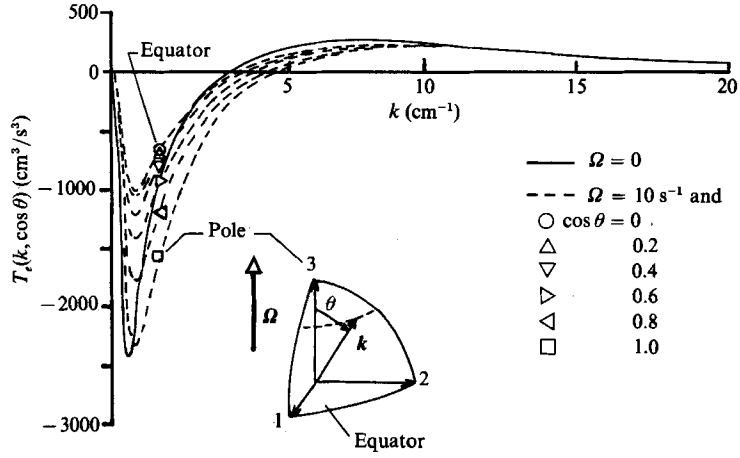

FIGURE 4. Initial angular distribution of the energy transfer $T_e(k, \cos\theta)$ for $\Omega = 10$ s^{-1} (isotropic initial data).

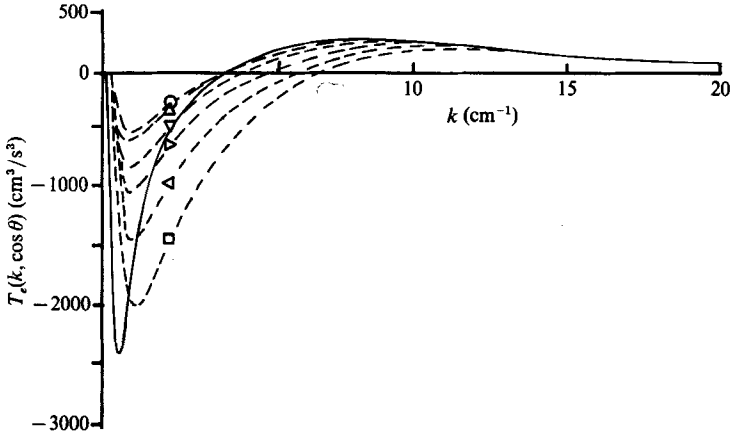

FIGURE 5. Initial angular distribution of the energy transfer $T_e(k, \cos\theta)$ for $\Omega = 20$ s^{-1} (isotropic initial data). Symbols as figure 4.

figures 4 and 5 for two values of the rotation rate ($\Omega = 10$ and 20 s^{-1}) corresponding to the initial Rossby numbers of 0.5 and 0.25 respectively.

The transfer appears strongly dependent on the cosine $\mu_k = \cos\theta$; it is compared with the corresponding isotropic transfer $T(k)$ for $\Omega = 0$ (full line). Considering the small wavenumber range ($T(k) < 0$), T_e appears strongly reduced for small values of μ_k ($\boldsymbol{k}$ more normal to $\boldsymbol{\Omega}$), and shifted rather than reduced for μ_k close to 1 ($\boldsymbol{k}$ more parallel to $\boldsymbol{\Omega}$).

This last behaviour leads to a non-isotropic distribution of $e(k, \mu_k, t)$. At the same time, an important anisotropy transfer $T_z = 4\pi k^2 (T_{ij} + T_{ij}^*) N_i^* N_j^*$ gives rise to a deviator $z(k, \mu_k, t)$.

The axisymmetric trend induced through the transfer term is less important in considering spectra integrated over a spherical shell, as shown in figure 6. Two contributions of $T_{ij}(\boldsymbol{k}, 0)$ are compared: the first one $S_{33}(k)$ corresponds to the longitudinal component $\varphi_{33}(k)$ of $\hat{\boldsymbol{U}}$ (integral of $\hat{U}_{33}$ $(\boldsymbol{k}, t)$ over a sphere of radius k) and the second $S_{11}(k)$ corresponds to the transverse component along a direction

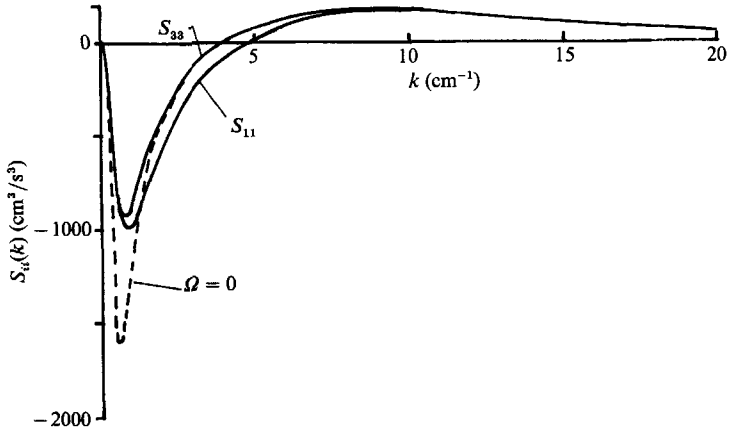

FIGURE 6. Initial nonlinear contributions $S_{ii}(k)$ to the integrated spectra $\varphi_{ii}(k)$ (isotropic initial data): -----, $S_{11} = S_{33}$ for $\Omega = 0$; ——, S_{11} and S_{33} for $\Omega = 10\ \mathrm{s}^{-1}$.

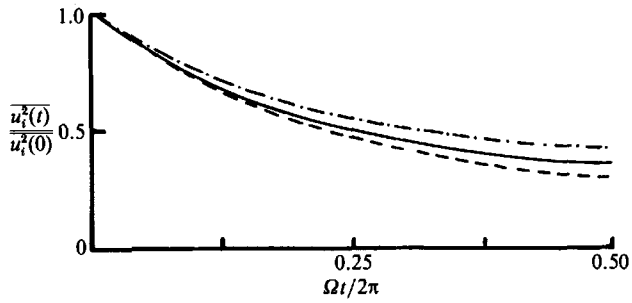

FIGURE 7. EDQNM evolution of the energy components (isotropic initial data): —·—·—, $\overline{u_3^2}$ for $\Omega = 10\ \mathrm{s}^{-1}$; ——, $\overline{u_1^2}$ for $\Omega = 10\ \mathrm{s}^{-1}$; -----, $\overline{u_3^2} = \overline{u_1^2}$ without rotation (here $\Omega t/2\pi$ is also calculated with $\Omega = 10$).

normal to $\boldsymbol{\Omega}$. By comparison to the corresponding (unique) component without rotation effect, we find a global reduction of the transfer from the large scales.

Considering now the evolution of one-point quantities, the non-isotropic manifestations are quite different on the Reynolds stresses and on the integral lengthscales. The decrease in the two components of the Reynolds stress tensor is slower in the presence of rotation, and the ratio $\overline{u_3^2}/\overline{u_1^2}$ grows moderately with time, as shown on figure 7. The increase in the three integral lengthscales $L_{33,3}$, $L_{33,1}$, $L_{11,1}$ as shown in figure 8, appears also moderately accentuated by the rotation; whereas the change in the behaviour of $L_{11,3}$ is particularly dramatic (very strong accentuation in the increase).

This behaviour of the four lengthscales has been observed by Bardina *et al.* (1985) and Dang & Roy (1985*b*) with a direct numerical simulation; however the increase in the ratio $\overline{u_3^2}/\overline{u_1^2}$ is very slight in these two simulations.

Moreover, a two-point closure model gives easier access to the angular dependence of the spectral quantities, such as e and z, and makes it possible to have a better understanding of the behaviours of $\overline{u_i^2}$ and $L_{ii,j}$ directly deduced by integration from such spectral quantities (equations (22), (23), (24)). In order to help the reader with an easier understanding of the analysis, the following explanations will be based on sketches rather than on the mathematical relationship.

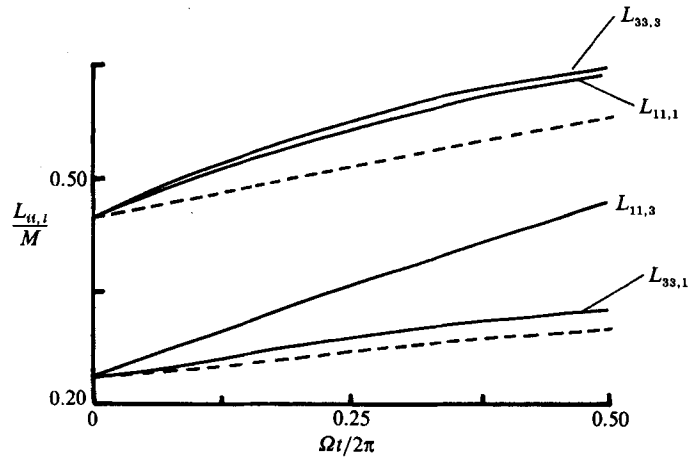

FIGURE 8. EDQNM evolution of the integral lengthscales (isotropic initial data): ——, $\Omega = 10\ \mathrm{s}^{-1}$; - - - - -, without rotation (here $\Omega t/2\pi$ is calculated with $\Omega = 10$).

Considering the spectral tensor $\hat{U}_{ij}(\boldsymbol{k}, t)$ at each point of a sphere of radius k, two kinds of anisotropy can be studied separately: first, the angular variability of the basic spectra e and z characterizes a 'directional anisotropy'; secondly, for a fixed orientation of $\boldsymbol{k}$, a complex value of z (modulus and argument) characterizes the anisotropic structure of $\hat{\boldsymbol{U}}$ which will be referred to as a 'local anisotropy'. Figure 9 presents the procedure adopted for visualizing these anisotropic features, following Bertoglio *et al.* (1979) and Cambon *et al.* (1985).

The ellipse shown in figure 9(*a*) represents the spectral tensor attached to a wave vector $\boldsymbol{k}$ and contained in the plane $P_{\boldsymbol{k}}$, according to figure 1; the view is normal to $\boldsymbol{k}$ so $\boldsymbol{e}^{(1)}$ and $\boldsymbol{e}^{(2)}$ are the horizontal and the vertical axes. The two axes of the ellipse coincide with the vectors $\phi^{(1)}\boldsymbol{a}$ and $\phi^{(2)}\boldsymbol{b}$, according to (8). Recall that $\boldsymbol{a}$ and $\boldsymbol{b}$ are the unit eigenvectors (or principal axes) of $\hat{\boldsymbol{U}}$ associated with the two non-zero eigenvalues (or principal components) ϕ^1 and ϕ^2 ($\phi^{(1)} \geqslant \phi^{(2)} > 0$). The magnitude of the spectral energy $e = \frac{1}{2}(\phi^{(1)} + \phi^{(2)})$ is represented by the size of the ellipse, whereas 'the local anisotropy' is represented by the eccentricity (or the flatness) of the ellipse. This last characteristic is emphasized by plotting a segment (the heavy line) which represents the vector $\boldsymbol{V}(z) = \frac{1}{2}(\phi^{(1)} - \phi^{(2)})\,\boldsymbol{a}$. This segment has length proportional to $|z| = \frac{1}{2}(\phi^{(1)} - \phi^{(2)})$ and its orientation is that of the principal axis of $\hat{\boldsymbol{U}}$ associated with the maximum principal component, so that $(\boldsymbol{e}^{(1)}, \boldsymbol{V}(z)) = \frac{1}{2}(\pi - \mathrm{Ang}\ z)$.

In figure 9(*b*–*e*), the local representations described above are viewed in perspective in the fixed frame of reference according to the definition of the local frame $(\boldsymbol{e}^{(1)}, \boldsymbol{e}^{(2)}, \boldsymbol{k}/k)$. These intrinsic representations of $\hat{\boldsymbol{U}}(\boldsymbol{k})$ are invariant by rotation around the vertical axis parallel to $\boldsymbol{\Omega}$. So the ellipse and the segment are plotted in the $P_{\boldsymbol{k}}$ plane at different points on a circle of radius k, corresponding to different angles $\theta = (\boldsymbol{k}, \boldsymbol{\Omega})$.

Four different situations, figures 9(*b*), 9(*c*), 9(*d*), 9(*e*), are considered, each one corresponding to a typical 'directional' or 'local' anisotropy. Below each spectral sketch, the corresponding contribution to the Reynolds stress tensor $\langle u_i u_j \rangle = \int \hat{U}_{ij}(\boldsymbol{k})\,\mathrm{d}\boldsymbol{k}^3$ is given. The lengths of the segments are proportional to the principal components of $\langle u_i u_j \rangle$ and their orientations are that of its principal axes, in accordance with previous tensorial representations.

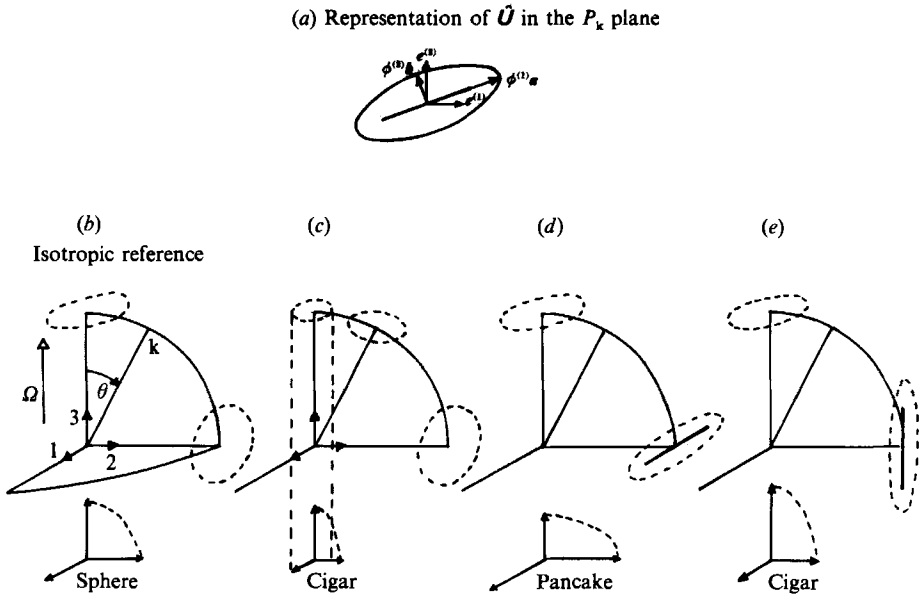

FIGURE 9. Representation of the spectral tensor and anisotropic features.

Figure 9(*c*) represents a pure directional anisotropy: $V(z)$ vanishes and the ellipse is a circle whose size depends on θ. In the isotropic case of reference (figure 9*b*) the size of the circle is the same for all the directions and the corresponding Reynolds stress tensor is spherical ($\overline{u_1^2} = \overline{u_2^2} = \overline{u_3^2}$). Now, we consider in figure 9(*c*) the anisotropic case where the spectral energy is smaller in the pole ($\theta = 0$, $\boldsymbol{k} \| \boldsymbol{\Omega}$) than in the equator ($\theta = \frac{1}{2}\pi$). The relative deficit of e in the polar zone, where $\hat{\boldsymbol{U}}$ lies in a horizontal plane (because of $\boldsymbol{k} \cdot \hat{\boldsymbol{u}} = 0$) diminishes the horizontal contributions to the Reynolds stress tensor. So a tendency for an axisymmetric Reynolds stress tensor of the 'cigar' type ($\overline{u_3^2} > \overline{u_1^2} = \overline{u_2^2}$) is created. In the opposite case, a relative dominance of the polar spectral energy (at $\theta = 0$) would create a tendency for a 'pancake' type ($\overline{u_3^2} < \overline{u_1^2} = \overline{u_2^2}$).

Figures 9(*d*) and 9(*e*) present the effects of a spectral anisotropy linked only to z, e being chosen independent of θ. The semi-axisymmetry (see table 1) and the Hermitian symmetry implies that $V(z)$ vanishes at the pole ($\theta = 0$) and is either horizontal or vertical at the equator, where its contribution appears crucial. A horizontal orientation of $V(z)$ at $\theta = \frac{1}{2}\pi$, as considered in the sketch 9(*d*) indicates the dominance of the horizontal mode ($\phi'_{11} = \phi^1 > \phi'_{22} = \phi^2$ at $\theta = \frac{1}{2}\pi$) and thus creates a tendency for a 'pancake' type. In the opposite case, a vertical orientation of $V(z)$, as considered in figure 9(*e*), which corresponds to a dominance of the vertical mode ($\phi'_{22} = \phi^1 > \phi'_{11} = \phi^2$ at $\theta = \frac{1}{2}\pi$) leads to a 'cigar' type.

Coming back to EDQNM results, figure 10(*a*) shows the shape of the energy spectrum $4\pi k^2 e(k, \cos\theta, t)$ for $\Omega t/2\pi = \frac{1}{2}$ at two extremal values of $\cos\theta$ (pole and equator). By comparison with the initial data ($4\pi k^2 e(k, \cos\theta, 0) = E(k)$) shown as a dashed line, it appears that the spectral energy decreases faster at the pole than at the equator. This relative concentration of the spectral energy is induced only by the transfer T_e, and creates a tendency for $\overline{u_3^2} > \overline{u_1^2}$, in accordance with the sketch 9(*c*).

Figure 10(*b*) exhibits the corresponding shape of z. Here $4\pi k^2 z$ is multiplied by k^2 in order to emphasize the contribution from the large wavenumbers. For each value

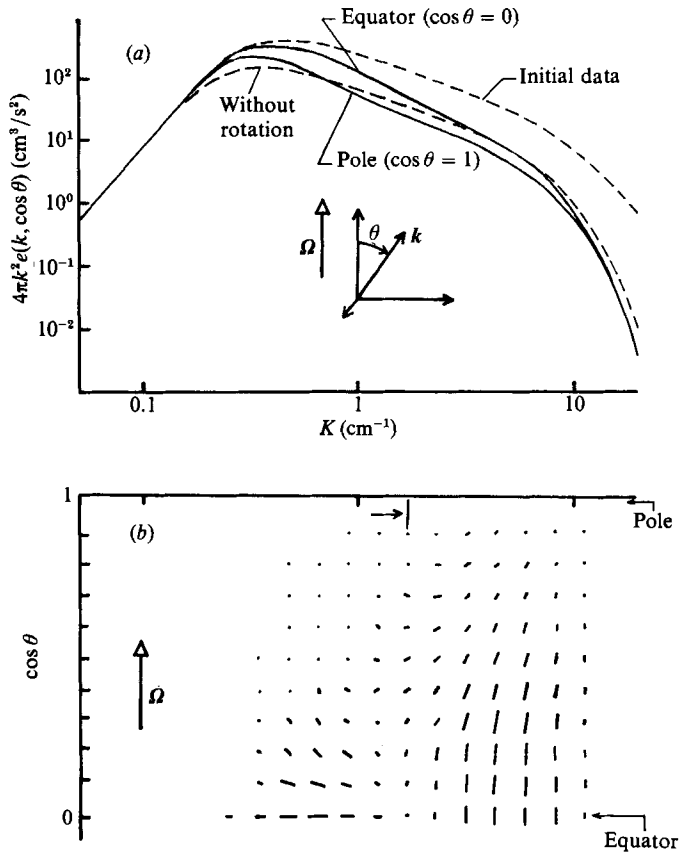

FIGURE 10. Angular distributions of the energy $e(k, \cos\theta)$ and the complex deviator $z(k, \cos\theta)$ at $\Omega t/2\pi = \frac{1}{2}$ (isotropic initial data).

of k and $\cos\theta$, the segment plotted represents the vector $4\pi k^4 \tilde{V}(z)$ in the same way as in figure 9(*a*). Two specific domains of k appear, the limit being indicated by an arrow.

For small wavenumbers, the segments of significant length (large anisotropic eddies) are more horizontal (perpendicular to $\boldsymbol{\Omega}$). This shape creates a tendency for $\overline{u_3^2} < \overline{u_1^2}$, in accordance with the sketch 9(*d*). Thus it appears that the contributions of e and z to the variation in the ratio $\overline{u_3^2}/\overline{u_1^2}$ are just the opposite. Moreover, if we compute the Reynolds stress tensor by integrating on a limited k-range (from 0 to the value corresponding to the arrow), we find the ratio $\overline{u_3^2}/\overline{u_1^2}$ to be nearly equal to the unity. The two kinds of anisotropy are therefore exactly balanced so as to ensure the sphericity of the Reynolds stress tensor.

At higher wavenumbers the segments are more vertical (parallel to $\boldsymbol{\Omega}$) and the contributions of e and z to the increase in the ratio $\overline{u_3^2}/\overline{u_1^2}$ are additive. Thus, taking into account the whole wavenumber range leads to an increase in the ratio $\overline{u_3^2}/\overline{u_1^2}$ as shown in figure 7.

Considering now the lengthscales $L_{11,3}$ and $L_{33,3}$; in accordance with (23) and (24) only the small-wavenumber range and the direction $\mu_k = \cos\theta = 0$ are relevant. The slower decay of e with rotation in this direction allows the faster increase of the two

lengthscales, whereas the spectacular increase in the ratio $L_{11,3}/L_{33,3}$ appears strongly linked with the horizontal orientation of the segments:

$$\frac{L_{11,3}}{L_{33,3}} = \frac{\int_0^\infty k\,\mathrm{d}k(e-z)|_{\mu_k=0}}{\int_0^\infty k\,\mathrm{d}k(e+z)|_{\mu_k=0}} \frac{1}{2}\frac{\overline{u_3^2}}{\overline{u_1^2}}, \quad V(z)\perp \boldsymbol{\Omega} \Rightarrow z<0.$$

Our analysis shows that the anisotropic features are masked when considering the Reynolds stress tensor, and emphasized when considering the lengthscales.

In addition, the underlying trends in wave space are consistent with two-dimensional features in the domain of large structures. Indeed, in theoretical two-dimensional isotropic turbulence, the spectral tensor becomes concentrated in the equatorial waveplane, so that

$$e(\boldsymbol{k}) = \frac{E(k)}{2\pi k}\delta(k_3); \quad z(\boldsymbol{k}) = -\frac{E(k)}{2\pi k}\delta(k_3); \quad V(z) = |z|\,\boldsymbol{e}^{(1)}.$$

In such a configuration the vertical mode $\phi'_{22} = \phi^{(2)} = e+z$ (at $k_3 = 0$) vanishes and zero values are found for both $\overline{u_3^2}$ and $L_{33,3}$. Here the two-dimensional trends appear simultaneously on e and z but we do not reach a purely two-dimensional state, where all the vertical quantities, such as $\overline{u_3^2}$, collapse.

If we discuss our results together with those of numerical simulations by Bardina *et al.* (1985) and Dang & Roy (1985*b*), we can point out the two following features:

(i) the Reynolds stress tensor remains quasi-spherical ($\overline{u_3^2} \approx \overline{u_1^2} = \overline{u_2^2}$) in direct numerical simulations, but a very weak trend $\overline{u_3^2} > \overline{u_1^2}$ is exhibited. Our computations emphasize the growth of this ratio only if a large wavenumber range is taken into account (effect of different Reynolds numbers?);

(ii) the behaviour of the four integral lengthscales is consistent between all the calculations, but the increase in $L_{11,3}$ is even more rapid in Dang & Roy's computation than in ours.

Note that the first term on the right-hand side in (11), associated with the initial data for triple correlations, was ignored in our computations. Indeed, it is usually stated in two-point closures that G_t^+ decays rapidly with time, so that $G_t^+ G_t^+ G_t^+$ is assumed to have only a transient effect, compared to

$$\int_0^t G_{t-t'}^+ G_{t-t'}^+ G_{t-t'}^+ \,\mathrm{d}t'.$$

This assumption has been numerically checked in the case treated here. The transfer T_e corresponding to this peculiar term appears not relevant for times exceeding a quarter of a revolution. Nevertheless, this energy transfer has an interesting structure, as shown in figure 11, at $\Omega t/2\pi = \frac{1}{8}$. By comparison with the initial isotropic energy transfer without rotation (dashed line), one observes a suppression of the transfer towards the small scales. Here the classical transfer between wavenumbers is wholly replaced by a directional drain from pole to equator (see arrow). Thus this peculiar contribution reinforces the directional effects already described, during a transient phase.

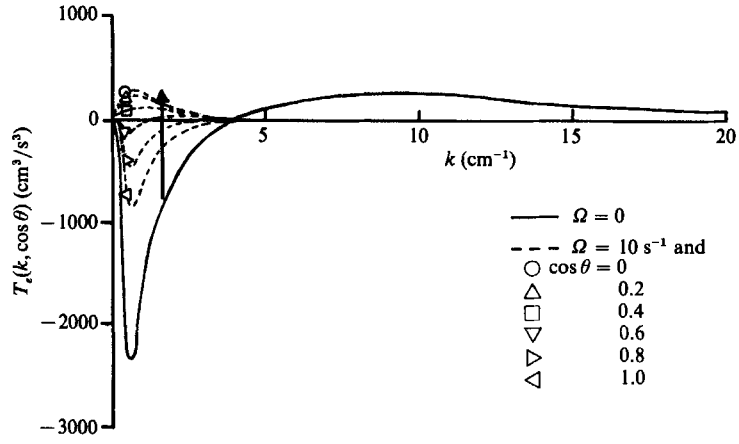

FIGURE 11 Angular distribution of the energy transfer $T_e(k, \cos\theta)$ for $\Omega = 10$ s^{-1} obtained from the linear evolution of the triple correlations at $\Omega t/2\pi = \frac{1}{8}$.

5. Conclusion

The main contribution of the two-point closure model described in this paper is a detailed analysis of the angular dependence induced by the rotation in the full three-dimensional energy and anisotropy spectra of turbulence. The classical statistical quantities can partly reflect this angular dependence, and some attempts to reach the angular variability of the spectral energy were proposed by Dang & Roy (1985*a*) in the case of strongly anisotropic initial data. Nevertheless, until now, no (fully three-dimensional) spectral tensor $\hat{U}_{ij}(\boldsymbol{k})$ derived from a direct numerical simulation has been presented in the case of an initial isotropic field evolving in the presence of solid-body rotation.

We have linked together the various (and apparently contradictory) trends observed in the behaviour of the Reynolds stress tensor and the integral lengthscales along with the typical angular-dependent spectral shape induced by the rotation.

Starting from isotropic initial data, an anisotropic shape is generated only by the triple correlations through the 'triadic Coriolis parameters' (24). Two manifestations of the two-dimensionality are identified: first the different values of the energy transfer $T_e(k, \cos\theta)$ with respect to $\cos\theta$, leads to a positive 'angular energy transfer' from the pole ($\cos\theta = 1$, $\boldsymbol{k} \| \boldsymbol{\Omega}$) to the equator ($\cos\theta = 0$, $\boldsymbol{k} \perp \boldsymbol{\Omega}$), thus tending to concentrate the spectral energy in the equatorial plane. Such a trend is compatible with the Proudman theorem: the asymptotic state that is predicted by the Proudman theorem corresponds in the spectral space to a vanishing of energy, except in the plane of wave vectors normal to $\boldsymbol{\Omega}$. Secondly, the horizontal mode of the spectral tensor becomes more important than the vertical one, in this equatorial plane, for low values of k. Such a trend is not predicted by the Proudman theorem. Considering only small values of k, the two previous behaviours are counterbalanced so as to ensure a quasi-isotropy (sphericity) of the Reynolds stress tensor, but the second leads to a strong increase in the ratio $L_{11,3}/L_{33,3}$ of the two longitudinal integral lengthscales. This last ratio appears as a relevant two-dimensionality criterion, in contrast to the criterion ($\overline{u_3^2}/\overline{u_1^2} < 1$) commonly used. In fact, the quasi-two-dimensionality requires a quite vertical orientation for the vortices, but does not necessarily exclude vertical motions.

In accordance with the results expected in the presence of rotation, the transfer of energy from small to high wavenumbers is inhibited. At the same time, the strong angular dependence of this effect leads to a draining of the energy from the pole to the equator. This result contradicts the assumption that the transfer is concentrated near the equator and blocked near the pole, as proposed by Bardina *et al.* (1985). The results concerning the angular distribution of $T_e(k, \cos\theta)$ and $e(k, \cos\theta)$ have been recently confirmed by numerical simulation (C. Teissèdre, private communication).

For a non-isotropic initial condition, the rotation also acts through linear terms in the equations governing the double correlations. Calculations of these linear effects show spectacular changes of the structure of the Reynolds stress tensor and of the lengthscales. These effects are transient: for the particular initial conditions that have been chosen, they are completely damped after half a revolution. These results could explain particular behaviour observed in experiments, such as that of Wigeland (1978), in which initial isotropy is not fulfilled (Cambon & Jacquin 1987).

Starting from the isotropic initial data, the moderate departure from the isotropy of the Reynolds stress tensor can be neglected and a $(k, \bar{\epsilon})$-model, corrected in an *ad hoc* way for rotation, is sufficient in practical modelling, as shown by Bardina *et al.* (1985) and Aupoix, Cousteix & Liandrat (1983). Note that the Aupoix model was supported by an isotropic EDQNM model, initially proposed by Cambon *et al.* (1981*b*). Nevertheless the behaviour of the lengthscales cannot be predicted by such simplified models.

Through a detailed investigation of the spectral mechanisms which underlie the behaviour of lengthscales and the Reynolds stress components, we have proposed a phenomenology of the transition from three-dimensional isotropic state to a quasi two-dimensional one for the case of rotating turbulence. The results concerning the physical quantities are in qualitative agreement with those of direct numerical simulations, but quantitative comparisons have still to be done. Experimental results available in the literature are too variable for this purpose. A new experiment is in progress at Onera which will provide results for detailed comparisons with the present theory.

The authors are grateful to J. Mathieu, O. Leuchter and B. Lakshminarayana for valuable discussions and for D. Jeandel for reading an earlier version of this paper.

REFERENCES

André, J. C. & Lesieur, M. 1977 Influence of helicity on the evolution of isotropic turbulence at high Reynolds number. *J. Fluid Mech.* **81**, 187–297.

Aupoix, B., Cousteix, J. & Liandrat, J. 1983 Effects of rotation on isotropic turbulence. In *Proc. 4th Symp. Turbulent Shear Flows, Karlsruhe* (ed. L. J. S. Bradbury *et al.*). Springer.

Bardina, J., Ferziger, J. H. & Rogallo, R. S. 1985 Effect of rotation on isotropic turbulence. *J. Fluid Mech.* **154**, 321–326.

Batchelor, G. K. 1953 *The Theory of Homogeneous Turbulence.* Cambridge University Press.

Bertoglio, J. P., Cambon, C., Jeandel, D. & Mathieu, J. 1979 Comparaison directe entre une modélisation directionnelle du tenseur spectral des corrélations doubles et une solution analytique dans le cas d'une turbulence homogène anisotrope. *C.R. Acad. Sci. Paris* **288** B, 473–475.

Cambon, C. 1982 Etude spectrale d'un champ turbulent incompressible soumis à des effets couples de déformation et de rotation imposés extérieurement. Thèse d'Etat, Université Lyon I.

Cambon, C., Bertoglio, J. P. & Jeandel, D. 1981*b* Spectral closures for homogeneous turbulence. *The 1980–81 AFOSR-HTTM-Stanford Conference on Complex Turbulent Flow*, vol. III, pp. 1307–1311.

CAMBON, C. & JACQUIN, L. 1985 Non isotropic aspects in homogeneous turbulence subjected to rotation. *Proc. Seventh AMS Symp. on Turbulence and Diffusion, Boulder.*

CAMBON, C. & JACQUIN, L. 1987 Spectral analysis of a three-dimensional homogeneous turbulence submitted to a solid body rotation. In *Advances in Turbulence* (ed. G. Comte-Bellot & J. Mathieu), pp. 170–175. Springer.

CAMBON, C., JEANDEL, D. & MATHIEU, J. 1981*a* Spectral modelling of homogeneous non-isotropic turbulence. *J. Fluid Mech.* **104**, 247–262.

CAMBON, C., TEISSÈDRE, C. & JEANDEL, D. 1985 Etude d'effets couplés de déformation et de rotation sur une turbulence homogène. *J. Méc. Théor. Appl.*, **4**, 629–657.

COMTE-BELLOT, G. & CORRSIN, S. 1971 Simple Eulerian time correlation of full and narrow-band velocity signals in grid-generated, 'isotropic' turbulence. *J. Fluid Mech.* **48**, 273–337.

CRAYA, A. 1958 Contribution à l'analyse de la turbulence associée à des vitesses moyennes. Thèse dans Publications Scientifiques et Techniques, Ministère de l'Air, France.

DANG, K. & ROY, PH. 1985*a* Numerical simulation of homogeneous turbulence. In *Proc. Workshop on Macroscopic Modelling of Turbulent Flows and Fluid Mixtures.* Springer.

DANG, K. & ROY, PH. 1985*b* Direct and large eddy simulation of homogeneous turbulence submitted to solid body rotation. In *Proc. 5th Symp. on Turbulent Shear Flows, Ithaca.*

GENCE, J. N. & MATHIEU, J. 1979 On the application of successive plane strains to grid-generated turbulence. *J. Fluid Mech.* **93**, 501–513.

GREENSPAN, H. P. 1968 *The Theory of Rotating Fluids.* Cambridge University Press.

HERRING, J. R. 1974 Approach of axisymmetric turbulence to isotropy. *Phys. Fluids* **17**, 859–872.

HOLLOWAY, G. & HENDERSHOTT, M. C. 1977 Stochastic closure for non-linear Rossby waves. *J. Fluid Mech.* **82**, 747–765.

HOPFINGER, E. J., BROWAND, F. K. & GAGNE, Y. 1982 Turbulence and waves in a rotating tank. *J. Fluid Mech.* **125**, 505–534.

ITSWEIRE, E., CHABERT, L. & GENCE, J. N. 1979 Action d'une rotation pure sur une turbulence homogène anisotrope. *C.R. Acad. Sci. Paris* **289 B**, 197–199.

LESIEUR, M. 1972 Décomposition d'un champ de vitesse non divergent en ondes d'hélicité. *Revue 'Turbulence'*. Observatoire de Nice.

ORSZAG, S. A. 1970 Analytical theories of turbulence. *J. Fluid Mech.* **41**, 262–386.

TOWNSEND, A. A. 1954 The uniform distortion of homogeneous turbulence. *Q. J. Mech. Appl. Maths*, **2**, 11000.

WIGELAND, R. A. 1978 Ph.D. thesis. Illinois Institute of Technology.